Data-Driven Gas Sensing Analysis of Copper Sulfide Films Modified with Manganese

Hayim Ch. Magid[1], Muna Ahmed Issa[2], Hanaa Kadem Essa[1], Wathiq Ayoub Taha Al Ramdhan[3] and Hadi Ahmed Hussin[1]

[1]*Department of Physics, College of Education, Mustansiriyah University, 10052 Baghdad, Iraq*
[2]*Quality Assurance and Performance Evaluation Department, Mustansiriyah University, 10052 Baghdad, Iraq*
[3]*Department of Medical Laboratory Techniques, Al-Manara College for Medical Sciences, 62001 Amarah, Iraq*
halhelfy@uomustansiriyah.edu.iq, muna.ahmed@uomustansiriyah.edu.iq, hanaa.kadhem@uomustansiriyah.edu.iq, Wathiq.alramdhan@uomanara.edu.iq, hadi.ahmed@uomustansiriayh.edu.iq

Keywords: Cu_2S: Mn, Thin Films, Plasma Jet, Nanostructure, Physical Properties.

Abstract: Cu_2S: Mn thin films were effectively prepared employing the plasma jet technique. The XRD patterns show a hexagonal structure. The particle size of all the films was revealed using an atomic force microscope (AFM) as spherically shaped grains of uniform size, tightly packed together. SEM images reveal Cu_2S: Mn nanostructures with crystallite nanorods. Plasma exposure time correlates with particle size (103-154.15 nm). Visible absorption spectra assure low absorption between 500 and 750 nm, revealing the film's excellent visibility in this range. The energy gap decreased from 2.57 eV (4 min) to 2.45 eV (12 min). The refractive index of Cu_2S films increases with increasing plasma exposure time. Cu_2S: Mn nanostructures, treated for 4, 8, and 12 minutes, showed varied resistance to NO_2 at 125°C, with the film treated for 4 minutes exhibiting the lowest resistance. Sensitivity of Cu_2S: Mn films to NO_2 decreases with increasing plasma exposure time, dropping notably at 450 ppm.

1 INTRODUCTION

The thin film industry would be significantly boosted by producing p-type semiconductors with high optoelectronic characteristics, mainly if their production can be achieved using currently available methods. Several materials, such as Cu_2S, have been identified as promising p-type candidates [1], [2]. The Cu_2S system is unique primarily because of its low cost and lack of toxicity [3], [4]. Cu_2S forms complicated structures, with Cu atoms in a mixed valence state in portions of its phase, and they have been the subject of much research over the years. Moreover, Cu_2S has fast ion conduction at high temperatures. Band edges exist at energies between 1.2 and 2.5 eV, according to several thorough absorption experiments on cuprous sulfide films with various stoichiometric compositions [5]. Additionally, Cu_2S transition band structure offers significant absorption coefficients (105 cm^{-1} for Cu_2S at 750 nm) [6]. Doping of semiconductors allowed them to be used widely in electrical and optical components [7]. Dopant ions are incorporated into the host semiconductor, enhancing its electrical conductivity and carrier concentration but decreasing transparency due to the increased absorption of free carriers [8], [9]. However, the charge scattering from ionized impurities at higher doping levels causes an increase in carrier concentration, which reduces mobility [10], [11]. The thin films were deposited using several processes, like plasma jet [12], pulsed laser deposition PLD [13]-[15], vacuum evaporation [16], SILAR [17], [18], ALD [19], CVD [20], and photochemical method [21]. In plasma jet, a simple deposition technique, the plasma plume interacts with a liquid of precursors to produce Cu_2S: Mn nanoparticles, which will later be deposited as thin films. Furthermore, owing to the possibilities of fine-tuning plasma parameters like time of exposure, flow rate, and other factors, this technique gives control over film thickness, stoichiometry, and nanostructure quality. It is a simple and cost-effective equipment and can be done at atmospheric pressure. We report on the role of plasma exposure time on the structural and optical properties of manganese-doped copper sulfide (Cu_2S: Mn) thin films grown by the cold plasma jet method. This work investigates gaseous Cu_2S: Mn nanostructured thin films subjected to varying durations of plasma treatment,

characterising the films based on crystallinity, optical band gap, and gas sensing performance.

2 EXPERIMENTAL

Nanostructured Cu_2S:Mn (0.05% wt.)thin films were prepared using a plasma jet system operating at atmospheric pressure. In this setup, argon gas was used as the working gas at a flow rate of 0.5 L/min, and a discharge voltage of 13 kV was applied between the electrodes. The plasma nozzle was positioned 2 cm above the surface of 10 mL of deionized water containing thiourea ($(NH_2)_2CS$) as a sulfur source and $MnCl_2$ as the manganese precursor. A high-purity copper plate (99.9%) was partially immersed in the liquid and served as the target electrode. The Ar plasma plume directly interacted with the liquid surface, producing reactive species that eroded the copper surface and initiated chemical reactions leading to the formation of Cu_2S: Mn nanoparticles. To investigate the effect of plasma exposure, the synthesis was conducted for 4, 8, and 12 minutes under identical conditions. The resulting colloidal suspensions exhibited a gradual color change, confirming nanoparticle formation. The obtained Cu_2S: Mn nanoparticles were deposited onto pre-cleaned glass substrates using the drop-casting technique. The samples were left to dry naturally at room temperature, forming visible thin films on the surface. The as-deposited films were then placed in a laboratory furnace at 150 °C for 30 minutes to enhance compactness, surface uniformity, and adhesion. This annealing process led to the formation of smooth, homogeneous, and well-adhered Cu_2S: Mn thin films, suitable for subsequent structural, optical, and gas-sensing analyses using XRD, AFM, SEM, and UV–Vis measurements.

3 RESULTS AND DISCUSSIONS

Figure 1 presents the X-ray diffraction patterns of the prepared films, confirming that the material consists of a polycrystalline Cu_2S phase. The diffraction peaks observed at specific 2θ positions correspond to characteristic crystallographic planes of Cu_2S, indicating the formation of nanostructured material. The identified peak positions are consistent with standard reference data for hexagonal Cu_2S (32-0348), confirming phase purity. It is also observed that with increasing plasma exposure time, the intensity of minor diffraction peaks increases, suggesting an improvement in crystallinity and structural ordering [22], [23], [24], [25].

The average crystallite size of Cu_2S:Mn was estimated using Scherrer's approach based on peak broadening in the XRD patterns [26], [27]. The calculated crystallite size for the film treated for 12 minutes ranges between 11.61 nm and 13.29 nm. The results indicate that crystallite size increases with longer plasma exposure time. This trend is attributed to improved atomic mobility and enhanced incorporation of Mn ions into the Cu_2S lattice. The close similarity between the ionic radii of Cu^{2+} and Mn^{2+} facilitates substitutional incorporation, which influences defect formation and grain growth. Small shifts in peak positions observed for Mn-doped Cu_2S at longer exposure times further confirm lattice modification effects. Similar behavior has been reported for Mn-doped CuS systems [28], [29].

The dislocation density was calculated using a standard relation based on crystallite size [30], [31]. This parameter represents the density of structural defects within the crystal and decreases as crystallite size increases.

The lattice strain was evaluated using a relation derived from XRD peak broadening [32], [33]. The obtained values of crystallite size, strain, and dislocation density are summarized in Table 1, while their variation with plasma exposure time is shown in Figure 2.

Overall, the results show that dislocation density decreases with increasing plasma exposure time, indicating a reduction in structural defects in Cu_2S:Mn films [34], [35]. This behavior is supported by the observed increase in peak intensity and reduction in strain. The increase in crystallite size is attributed to improved Mn incorporation and reduced defect density during longer plasma treatment. Mn atoms are likely to occupy dislocation sites within the lattice, which helps relieve internal stress and stabilize the structure [36], [37]. As a result, both strain and dislocation density decrease simultaneously, demonstrating a strong interdependence between these microstructural parameters, consistent with previously reported results for Mn-doped Cu_2S systems [38], [39].

Table 1: D, E_g, and structural coefficient at different plasma exposure times.

Specimen	2 θ (°)	(hkl) Plane	FWHM (°)	E_g (eV)	D (nm)	δ (× 10^{14}) (lines/m^2)	ε (× 10^{-4})
Cu_2S: Mn at t=4 min	30.91	200	0.708	2.57	11.61	74.14	29.85
Cu_2S: Mn at t=8 min	30.88	200	0.660	2.51	12.49	64.08	27.75
Cu_2S: Mn at t=12 min	30.86	200	0.620	2.45	13.29	56.07	26.07

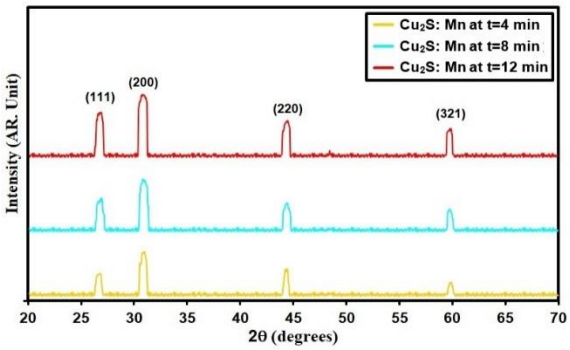

Figure 1: XRD styles of Cu_2S: Mn films.

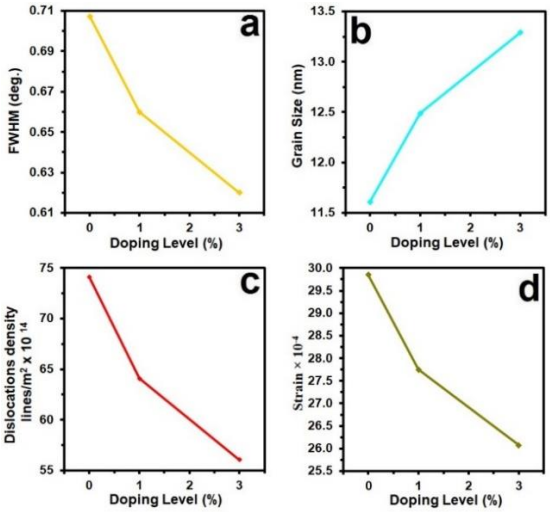

Figure 2: FWHM (a) D (b) δ (c) ε (d) of Cu_2S: Mn films.

The surface morphology of the Cu_2S:Mn thin films was investigated at the nanoscale using atomic force microscopy (AFM). Figures 3 (a1, b1, and c1) present the three-dimensional surface topography of the films deposited on glass substrates. Image processing software was used to estimate the average grain size and surface roughness. The AFM results show that all films consist of nearly spherical, uniformly distributed, and densely packed grains. The surfaces are continuous and fully cover the substrates without visible cracks, voids, or discontinuities.

The average grain size ranges from approximately 42.17 nm to 73.86 nm, showing a clear dependence on plasma exposure time [40], [41]. The root mean square roughness values are 2.27 nm, 2.84 nm, and 5.88 nm for films treated for 4, 8, and 12 minutes, respectively. Overall, the surface roughness varies systematically with increasing plasma exposure time, as summarized in Table 2 (PAFM). The observed changes indicate that longer plasma treatment leads to finer and more uniformly distributed grains, which is consistent with the structural improvements observed in the XRD analysis.

Optical transmittance was determined experimentally based on the ratio between transmitted and incident light intensities. This parameter is typically expressed as a percentage.

Figure 4 presents the transmittance spectra of Cu_2S:Mn thin films prepared at different plasma exposure times. In the wavelength range of approximately 600–800 nm, the transmittance values lie between 70% and 85%. The increase in transmittance is associated with reduced surface roughness and smaller crystallite size, indicating improved optical quality of the films.

Figure 5 shows the absorbance spectra of Cu_2S:Mn films prepared under different plasma exposure conditions. Lower absorbance is observed at shorter plasma exposure times, while the sample treated for 12 minutes shows increased absorbance in the visible region near 600 nm. These results indicate that the optical absorption behavior strongly depends on plasma exposure time, reflecting changes in microstructure and electronic properties of the films [46], [47].

Table 2: P_{AFM} of Cu_2S: Mn films.

Sample	P_{av} (nm)	R_a (nm)	RMS (nm)
Cu_2S: Mn at t=4 min	42.17	4.27	2.27
Cu_2S: Mn at t=8 min	68.49	6.10	2.84
Cu_2S: Mn at t=12 min	73.86	8.79	5.88

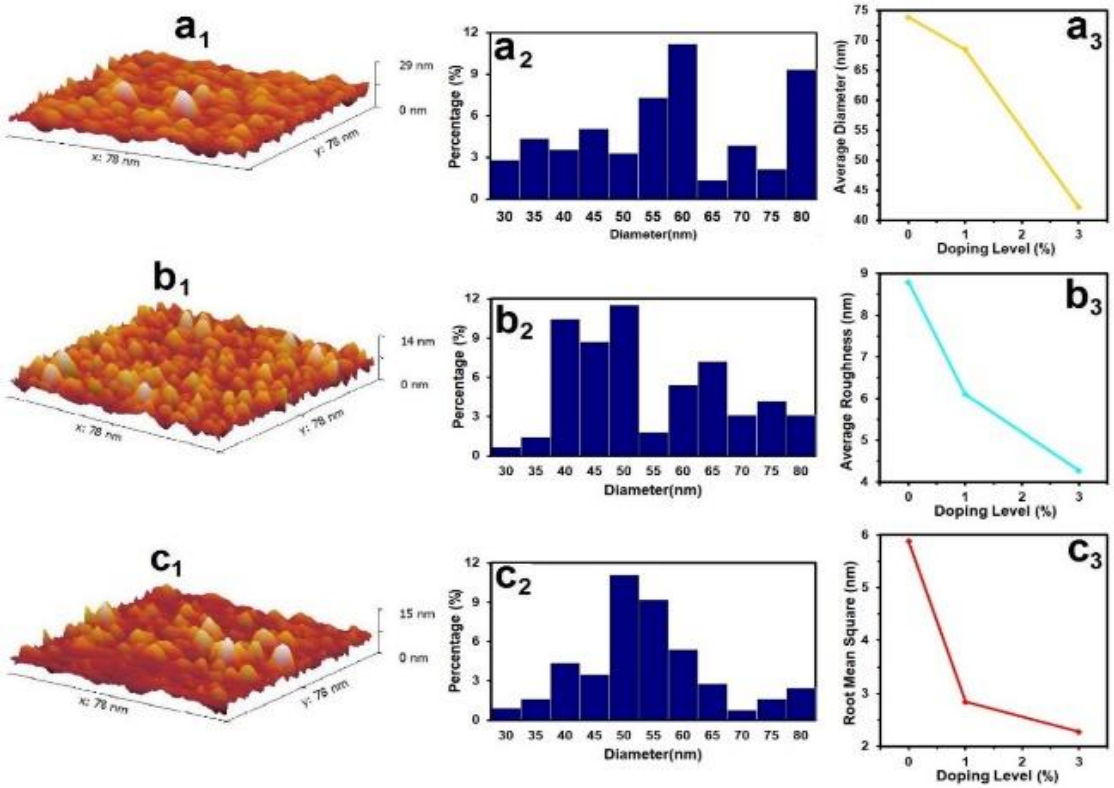

Figure 3:AFM images, granularly distributed, and diversity of P_{av}.

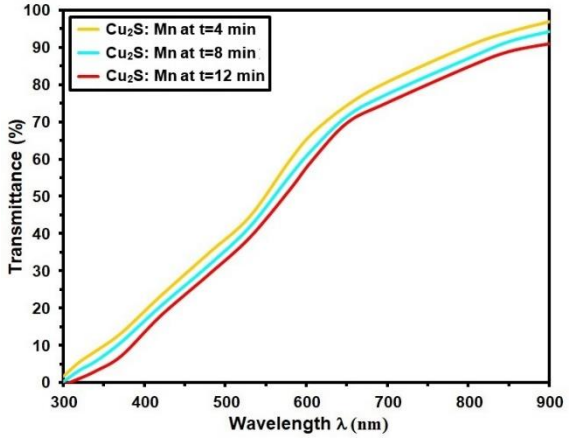

Figure 4: T with wavelength of Cu_2S: Mn films.

Using relation [5], the absorption coefficient was determined from the absorbance and the film thickness in the strong absorption region of the films [48], [49]. Figure 6 illustrates how the absorption coefficient for Cu2S:Mn thin films varies with wavelength. The absorption edge shifts toward longer wavelengths as the plasma exposure time increases. This strong absorption is a key reason for potential applications in solar energy harvesting and photovoltaic systems. The observed behavior is attributed to a shift of donor levels toward the conduction band, while the reduction in energy is linked to the increase in crystallite size [50], [51]. The absorption coefficient increases from 3.2×10^4 to 3.9×10^4 cm^{-1} as the plasma exposure time is increased from 4 to 12 minutes.

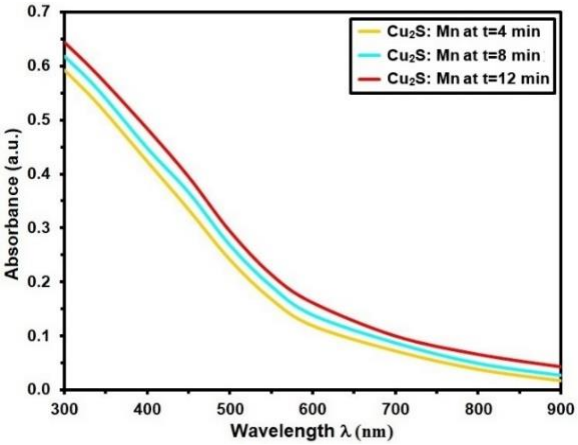

Figure 5: Absorbance with wavelength of Cu_2S: Mn films.

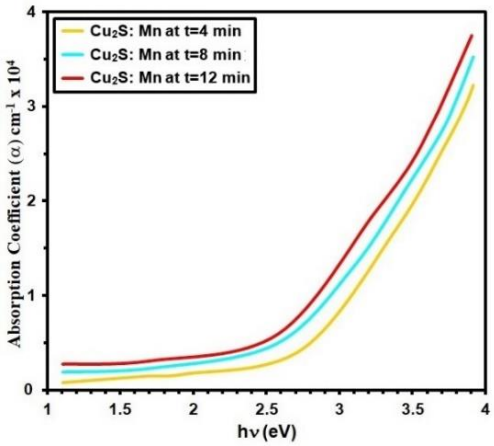

Figure 6: α versus hν for the Cu_2S: Mn films at different plasma exposure times.

The optical band gap was determined using Tauc's model [52], [53], which relates the absorption coefficient and photon energy for allowed direct transitions. The corresponding plots for different plasma exposure times are shown in Figure 8. The optical band gap values of Cu2S:Mn nanostructures decrease from 2.57 eV to 2.45 eV as the plasma treatment duration increases. Figure 7 shows that the energy gap narrows with increasing plasma exposure time due to the growth in crystallite size. As a result, absorption increases when the band gap decreases, and the optical absorption edge shifts toward longer wavelengths [54], [55].

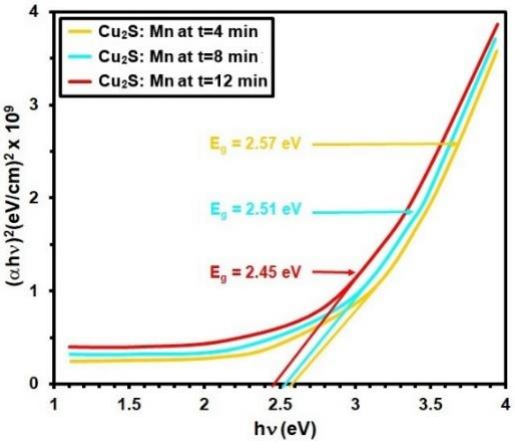

Figure 7: $(\alpha h\nu)^2$ versus hν for the Cu_2S: Mn films at different plasma exposure times.

The refractive index was evaluated using a relation based on reflectance data [56], [57], while the extinction coefficient was calculated using a relation involving the absorption coefficient and wavelength [58], [59]. The variation of the refractive index is shown in Figure 8. It generally increases with increasing plasma exposure time and decreases with wavelength, indicating that Cu2S:Mn films possess a relatively high refractive index compared to other semiconductors. The spectral dependence of the extinction coefficient is shown in Figure 9. It behaves similarly to the refractive index, increasing in a consistent manner with longer plasma treatment times from 4 to 12 minutes [60], [61]. This behavior is explained by differences in ionic radii between Cu^{2+} and Mn^{2+}, which can lead to the formation of additional defect states [62]. Optical properties are also influenced by factors such as oxygen deficiency, impurity centers, and surface roughness [63].

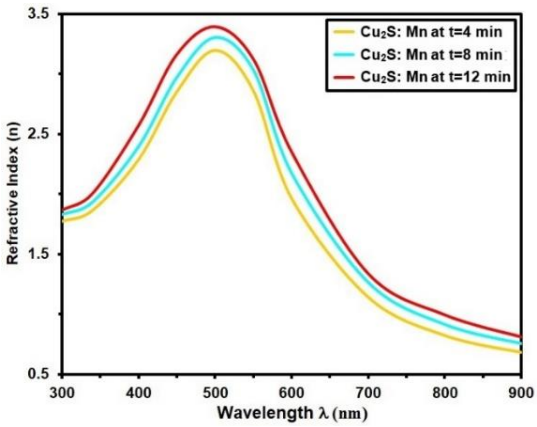

Figure 8: n for Cu_2S: Mn films.

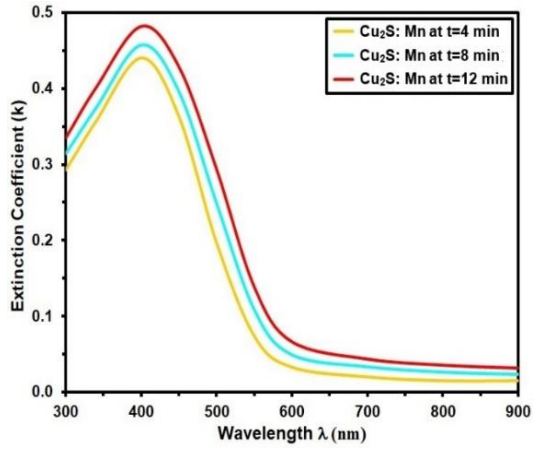

Figure 9: k for Cu_2S: Mn films.

The gas-sensing properties of Cu_2S: Mn nanostructures were studied for NO_2, an oxidizing and reducing gas, at 125°C. The resistance changes of Cu_2S: Mn films under exposure to 450 ppm of oxidising gas (NO_2) is depicted in Figure 10. The film

treated for 4 minutes showed the lowest resistance due to high roughness and increased surface area observed in AFM and SEM analysis. Electrical resistance data confirmed this. In contrast, the film treated for 12 minutes exhibited the highest resistance, which is attributed to electron extraction from ionized donors, thereby increasing the hole density at the gas-solid interface [64], [65]. The potential barrier for electrons decreased with rising oxygen ion density on the surface, impacting the electrical resistivity influenced by adsorbed oxygen ions. The introduction of NO_2 altered the ion concentration, leading to reduced resistance [66], [67].

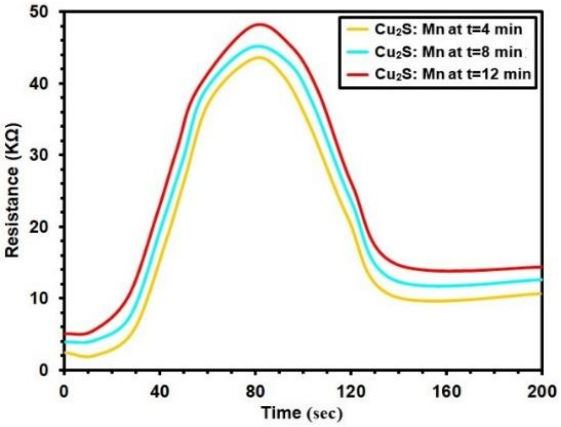

Figure 10: The resistance variation over time for Cu_2S: Mn films.

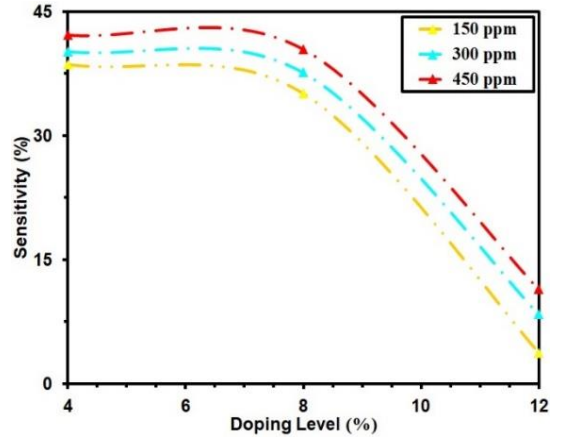

Figure 11: The sensitivity of Cu_2S: Mn films.

The sensitivity was calculated based on the change in electrical resistance between gas and air environments [68], [69]. Rg and Ra represent the resistance of the film in gas and air, respectively. Figure 11 shows the influence of plasma exposure time on NO_2 gas sensitivity of Cu2S:Mn thin films. The sensitivity decreases with increasing plasma exposure time, which is attributed to charge carrier recombination processes [70]. The sensitivity also decreases as NO_2 concentration increases (150 ppm, 300 ppm, and 450 ppm) [60]–[62]. In addition, films treated for longer durations (8 and 12 minutes) show lower sensitivity compared to the 4-minute sample, indicating reduced gas response with extended plasma exposure [71]–[74].

4 CONCLUSIONS

The plasma jet technique has effectively synthesized Cu_2S: Mn. Cu_2S: Mn nanofilms were shown to have a hexagonal structure by XRD analysis, with crystallite sizes ranging from 11.21 nm for the film treated for 4 minutes to 13.28 nm for the film treated for 12 minutes. The average grain size of the deposition films AFM micrographs is between 73.86 and 42.17 nm, and the (RMS) values of the thin film surface roughness decrease as the plasma exposure time increases, from 5.88 nm to 2.84 nm and 2.27 nm, respectively. SEM images depict Cu_2S nanostructures with defined crystallite nanorods. Increasing plasma exposure time enhances particle size (103 nm to 154.15 nm). The results of the optical study demonstrated that when the plasma treatment time was raised from 4 to 12 minutes, the absorption coefficient increased from 3.2×10^4 to 3.9×10^4 cm^{-1}. The obtained optical bandgap values of Cu_2S: Mn nanostructures decreased from (2.57 to 2.45) eV. Cu_2S: Mn nanostructures, treated for 4, 8, 12 minutes, showed varied resistance to NO_2 at 125°C, with the film treated for 4 minutes exhibiting the lowest resistance. Sensitivity to NO_2 decreases with increasing plasma exposure time.

ACKNOWLEDGMENTS

Mustansiriyah University and Alnukhba University College supported the prevention work.

REFERENCES

[1] C. Cruz-Vazquer and M. B. Inoue, “Characterization of new copper sulphide materials,” Superficesy Vacio, vol. 9, pp. 219-221, 1999.

[2] S. V. Bague, “Growth and Characterization of CuxS (x = 1.0; 1.76 and 2.0) thin films grown by solution growth,” Journal of Physics and Chemistry of Solids, vol. 68, pp. 1623-1629, 2007.

[3] L. Reijnen, B. Meester, A. Goossens, and J. Schoonman, Mater. Sci. Eng. C Biomim. Mater. Sens. Syst., vol. 19, p. 311, 2002.

[4] R. C. Maity, "Synthesis and characterization of aluminium doped CdO thin films by Sol-gel process," Sol. Energy Mater. & Sol. Cell, vol. 90, pp. 597-606, 2006.

[5] A. S. Al-Shammari, A. F. Mulla, and A. M. Dhafiri, "Preparation and characterization of chlorine doped Cadmium sulphide thin films and their applications," M.Sc. thesis, Dept. Physics and Astronomy, King Saud Univ., Saudi Arabia, 2005.

[6] X. Xu, J. Bullock, L. T. Schelhas, E. Z. Stutz, J. J. Fonseca, M. Hettick, V. L. Pool, K. F. Tai, M. F. Toney, X. Fang, A. Javey, L. H. Wong, and J. W. Ager, "Chemical bath deposition of p-type transparent, highly conducting (CuS)x:(ZnS)1–x nanocomposite thin films and fabrication of Si heterojunction solar cells," Nano Lett., vol. 16, pp. 1925–1932, 2016.

[7] M. Dhanasekar, G. Bakiyaraj, and K. Rammurthi, International Journal of Chem Tech Research, vol. 7, no. 3, p. 1057, 2015.

[8] B. D. Cullity, Elements of X-Ray Diffraction, 1st ed. Reading, MA, USA: Addison-Wesley Publishing Company Inc., 1956.

[9] S. H. Chaki, J. P. Tailor, and M. P. Deshpande, "Synthesis and Characterizations of Undoped and Mn Doped CuS Nanoparticles," Advanced Science Letters, vol. 20, pp. 959–965, 2014.

[10] J. Henry, T. Daniel, V. Balasubramanian, K. Mohanraj, and G. Sivakumar, "Electrical and optical properties of Sb-doped Cu2Se thin films deposited by chemical bath deposition," Phase Transitions, vol. 93, no. 8, 2020.

[11] S. Bornholdt, M. Wolter, and H. Kersten, "Characterization of an atmospheric pressure plasma jet for surface modification and thin film deposition," The European Physical Journal D, vol. 60, no. 3, pp. 653-660, 2010.

[12] M. A. Issa and K. A. Aadim, "Study the structural and optical properties of Zinc Oxide prepared by pulse laser deposition," J Opt, 2024, [Online]. Available: https://doi.org/10.1007/s12596-024-02034-2.

[13] M. A. Issa and K. A. Aadim, "Optical and structural characterization of ZnO:NiO nano composite prepared by pulsed laser deposition method," J Opt, vol. 54, pp. 2357–2362, 2025, [Online]. Available: https://doi.org/10.1007/s12596-024-01951-6.

[14] M. A. Issa and K. A. Aadim, "Influence Of Laser Energy On Structural And Optical Properties Of ZnO(x):NiO(1−x) Films Prepared By Pulse Laser Deposition," J Opt, 2024, [Online]. Available: https://doi.org/10.1007/s12596-024-02212-2.

[15] L. Isac, L. Andronic, A. Enesca, and A. Duta, "The Influence of Light Irradiation on the Photocatalytic Degradation of Organic Pollutants," J. Photochem. Photobiol. A Chem., vol. 252, pp. 53–59, 2013.

[16] A. L. Abdelhady, K. Ramasamy, M. A. Malik, P. O'Brien, S. J. Haigh, and J. Raftery, "New Routes to Copper Sulfide Nanostructuers and Thin Films," J. Mater. Chem., vol. 21, pp. 17888–17895, 2011.

[17] S. Sartale and C. Lokhande, "Growth of copper sulphide thin films by successive ionic layer adsorption and reaction (SILAR) method," Mater. Chem. Phys., vol. 65, pp. 63–67, 2000.

[18] J. Johansson, J. Kostamo, M. Karppinen, and L. Niinisto, "Growth of Cu2S thin films by atomic layer deposition using Cu(dmamb)2 and H2S," J. Mater. Chem., vol. 12, pp. 1022–1026, 2002.

[19] H. Pathan, J. Desai, and C. Lokhande, "Modified chemical deposition and physico-chemical properties of copper sulphide (Cu2S) thin films," Appl. Surf. Sci., vol. 202, pp. 47–56, 2002.

[20] H. J. Kwon, S. Thanikaikarasan, T. Mahalingam, K. H. Park, C. Sanjeeviraja, and Y. D. Kim, Journal of Materials Science: Materials in Electronics, vol. 19, p. 1086, 2008.

[21] J. Simmons and K. S. Potter, Optical Materials, 1st ed. New York, NY, USA: Academic Press, 1999.

[22] M. Ramya and S. Ganesan, "Study on current conduction mechanism in evaporated Cu2S thin films," Optoelectronics and Advanced Materials-Rapid Communications, vol. 5, pp. 936-942, 2011.

[23] J. Li, H. Zhao, X. Chen, H. Jia, and Z. Zheng, "In situ fabricate Cu2S thin film with hierarchical petal-like nanostructures," Materials Research Bulletin, vol. 48, pp. 2940-2943, 2013.

[24] C. Jiang, W. Zhang, G. Zou, L. Xu, W. Yu, and Y. Qia, "Hydrothermal fabrication of copper sulfide nanocones and nanobelts," Materials Letters, vol. 59, pp. 1008-1011, 2005.

[25] C. Y. Su, D. K. Mishra, C. Y. Chiu, and J. M. Ting, "Effects of Cu2S sintering aid on the formation of CuInS2 coatings from single crystal Cu2In2O5 nanoparticles," Surface and Coatings Technology, vol. 231, pp. 517-520, 2013.

[26] P. More, S. Dhanayat, K. Gattu, S. Mahajan, D. Upadhye, and R. Sharma, "Annealing effect on Cu2S thin films prepared by chemical bath deposition," AIP Conference Proceedings, vol. 1728, art. no. 020489, 2016.

[27] D. Chakraborty, S. Kaleemulla, N. M. Rao, et al., "Synthesis and magnetic properties of (Fe, Sn) co-doped In2O3 nanoparticles," J Mater Sci: Mater Electron., vol. 28, pp. 18977–18985, 2017.

[28] V. B. Ghanwat, S. S. Mali, C. S. Bagade, et al., "Thermoelectric properties of indium(III)-doped copper antimony selenide thin films deposited using a microwave-assisted technique," Ener Technol., vol. 4, pp. 835–842, 2016.

[29] S. Valencia, J. M. Martin, and G. Restepo, "Study of the bandgap of synthesized Titanium Dioxide nanoparticles using the sol-gel method and a hydrothermal treatment," The Open Mater. Sci. Journ., vol. 4, pp. 9-14, 2010.

[30] A. M. Muhammed, A. E. Ibrahim, and R. A. Ismail, "Study an Effect of Thiourea Concentration on the Structural, Optical and Electrical Properties of (Cu2S) film Prepared by Chemical Bath Deposition (CBD)," Kirkuk Univ. J.-Sci. Stud., vol. 14, pp. 97–115, 2019.

[31] D. M. Shaker, R. R. Ahmed, A. M. Mohammad, T. H. Mubarak, and I. H. Mohamed, "Synthesis and Characterization of CoZnFe2O4 Ferrite Nanoparticles by Co-precipitation Method for Biomedical Applications," Passer Journal of Basic and Applied Sciences, vol. 6, no. 2, pp. 488–493, 2024.

[32] R. S. Ali, H. S. Rasheed, N. F. Habubi, and S. S. Chiad, "Synthesis and characterization of manganese-doped FeS2 thin films via chemical spray pyrolysis," Chalcogenide Letters, vol. 20, no. 1, pp. 63–72, 2023.

[33] J. Podder, R. Kobayashi, and M. Ichimura, "Photochemical deposition of CuxS thin films from aqueous solutions," Thin Solid Films, vol. 472, pp. 71–75, 2004.

[34] A. J. Mawat, M. H. Al-Timimi, W. H. Albanda, and M. Z. Abdullah, "Morphological and optical properties of Mg1-xCdSx nanostructured thin films," AIP Conference Proceedings, vol. 2475, art. no. 090019, 2023.

[35] R. A. Ismail, A. E. Al-Samarai, and A. M. M. Ali, "Effect of molar concentration of CuCl2 on the characteristics of Cu2S film," Opt. Quantum Electron., vol. 52, pp. 1–14, 2020.

[36] M. B. Jumaa, T. H. Mubaraka, and A. M. Mohammad, "Study of the structural, magnetic and electrical properties of Co1.2Fe1.8O4 nanoferrites," AIP Conference Proceedings, vol. 2475, art. no. 090014, 2023.

[37] P. Kosoljitkul, P. Rakkroekkong, and P. Vas-Umnuay, "Parameter-controllable microchannel reactor for enhanced deposition of copper sulfide thin films," Thin Solid Films, vol. 646, pp. 150–157, 2018.

[38] Y.-W. Su, B. K. Paul, and C.-H. Chang, "Investigation of CdS nanoparticles formation and deposition by the continuous flow microreactor," Appl. Surf. Sci., vol. 472, pp. 158–164, 2019.

[39] A. S. Al Rawas, M. Y. Slewa, B. A. Bader, N. F. Habubi, and S. S. Chiad, "Physical characterization of nickel doped nanostructured TiO2 thin films," Journal of Green Engineering, vol. 10, no. 9, pp. 7141-7153, 2020.

[40] P. V. Nho, P. H. Ngan, N. Q. Tien, and H. D. Viet, "Preparation and characterization of low resistivity CuS films using spray pyrolysis," Chalcogenide Lett., vol. 9, pp. 397–402, 2012.

[41] F. Zhuge, X. Li, X. Gao, X. Gan, and F. Zhou, "Synthesis of stable amorphous Cu2S thin film by successive ion layer adsorption and reaction method," Mater. Lett., vol. 63, pp. 652–654, 2009.

[42] J. G. Omwoyo, "Characterization of Cu2S/SnO2: F pn Junction for Solar Cell Applications," M.Sc. thesis, Kenyatta Univ., Nairobi, Kenya, 2019.

[43] F. G. Hone and T. Abza, "Short Review of Factors Affecting Chemical Bath Deposition Method for Metal Chalcogenide Thin Films," Int. J. Thin Film. Sci. Technol., vol. 8, no. 3, 2019.

[44] N. K. Allouche, T. Ben Nasr, C. Guasch, and N. K. Turki, "Optimization of the synthesis and characterizations of chemical bath deposited Cu2S thin films," Comptes Rendus. Chim., vol. 13, pp. 1364–1369, 2010.

[45] F. G. Hone and F. B. Dejene, "Cationic concentration and pH effect on the structural, morphological and optical band gap of chemically synthesized lead sulfide thin films," J. Mater. Res. Technol., vol. 8, pp. 467–474, 2019.

[46] F. Kırmızıgül, E. Güneri, and C. Gümüş, "Effects of different deposition conditions on the properties of Cu2S thin films," Philos. Mag., vol. 93, pp. 511–523, 2013.

[47] M. Patil, D. Sharma, A. Dive, S. Mahajan, and R. Sharma, "Study of various synthesis techniques of nanomaterials," in AIP Conference Proceedings, Melville, NY, USA: AIP Publishing LLC, 2018.

[48] J. K. Hedlund, T. G. Estrada, and A. V. Walker, "Chemical Bath Deposition of Copper Sulfide on Functionalized SAMs: An Unusual Selectivity Mechanism," Langmuir, vol. 36, pp. 3119–3126, 2020.

[49] A. A. Kamil, N. A. Bakr, T. H. Mubaraka, and J. Al-Zanqanawee, "Synthesis and study of the optical and structural properties of Au and Ag nanoparticles by pulsed laser ablation (PLAL) technique," Digest Journal of Nanomaterials and Biostructures, vol. 16, no. 4, pp. 1219–1226, 2021.

[50] E. H. Hadi, M. A. Abbsa, A. A. Khadayeir, Z. M. Abood, N. F. Habubi, and S. S. Chiad, "Effects of Mn doping on the characterization of nanostructured TiO2 thin films deposited via chemical spray pyrolysis method," Journal of Physics: Conference Series, vol. 1664, no. 1, 2020.

[51] A. N. Kassim, H. S. Min, L. K. Siang, and S. A. Nagalingam, "SEM, EDAX and UV-Visible studies on the properties of Cu2S thin films," Chalcogenide Lett., vol. 8, pp. 405–410, 2011.

[52] H. Li, Y. Wang, J. Jiang, Y. Zhang, Y. Peng, and J. Zhao, "CuS Microspheres as High-Performance Anode Material for Na-ion Batteries," Electrochimica Acta, vol. 247, pp. 851–859, 2017.

[53] S. K. Muhammad, E. S. Hassan, K. Y. Qader, K. H. Abass, S. S. Chiad, and N. F. Habubi, "Effect of vanadium on structure and morphology of SnO2 thin films," Nano Biomedicine and Engineering, vol. 12, no. 1, pp. 67-74, 2020.

[54] K. Guo, X. Chen, J. Han, and Z. Liu, "Synthesis of ZnO/Cu2S core/shell nanorods and their enhanced photoelectric performance," J. Sol-Gel Sci. Technol., vol. 72, pp. 92–99, 2014.

[55] R. A. Ismail, A.-M. E. Al-Samarai, and A. M. Muhammed, "High-performance nanostructured p-Cu2S/n-Si photodetector prepared by chemical bath deposition technique," J. Mater. Sci. Mater. Electron., vol. 30, pp. 11807–11818, 2019.

[56] P. Makuła, M. Pacia, and W. Macyk, "Investigation of optical properties of the PbS/CdS thin films by thermal Evaporation," J. Electron Devices, vol. 12, pp. 761–766, 2012.

[57] P. Makuła, M. Pacia, and W. Macyk, "How to Correctly Determine the Band Gap Energy of Modified Semiconductor Photocatalysts Based on UV–Vis Spectra," ACS Publications, Washington, DC, USA, 2018.

[58] B. A. Bader, S. K. Muhammad, A. M. Jabbar, K. H. Abass, S. S. Chiad, and N. F. Habubi, "Synthesis and Characterization of Indium-doped CdO Nanostructured Thin Films: a Study on Optical, Morphological, and Structural Properties," J. Nanostruct., vol. 10, no. 4, pp. 744-750, 2020.

[59] F. Ouachtari, A. Rmili, B. Elidrissi, A. Bouaoud, H. Erguig, and P. Elies, "Influence of Bath Temperature, Deposition Time and S/Cd Ratio on the Structure, Surface Morphology, Chemical Composition and Optical Properties of CdS Thin Films Elaborated by Chemical Bath Deposition," J. Mod. Phys., vol. 02, pp. 1073–1082, 2011.

[60] M. Sangamesha, K. Pushapalatha, and G. Shekar, "Effect of concentration on structural and optical properties of CuS thin films," Int. J. Pure Appl. Res. Eng. Technol., vol. 2, p. 227, 2013.

[61] P. Vas-Umnuay and C.-H. Chang, "Growth Kinetics of Copper Sulfide Thin Films by Chemical Bath Deposition," ECS J. Solid State Sci. Technol., vol. 2, pp. P120–P129, 2013.

[62] H. A. Hussin, R. S. Al-Hasnawy, R. I. Jasim, N. F. Habubi, and S. S. Chiad, "Optical and structural properties of nanostructured CuO thin films doped by Mn," Journal of Green Engineering, vol. 10, no. 9, pp. 7018-7028, 2020.

[63] H. Xu, J. Dong, and C. Chen, "One-step chemical bath deposition and photocatalytic activity of Cu2O thin films with orientation and size controlled by a chelating agent," Mater. Chem. Phys., vol. 143, pp. 713–719, 2014.

[64] M. Yu, T. I. Draskovic, and Y. Wu, "Understanding the crystallization mechanism of delafossite CuGaO2 for controlled hydrothermal synthesis of nanoparticles and nanoplates," Inorg. Chem., vol. 53, pp. 5845–5851, 2014.

[65] S. Rondiya, A. Rokade, B. Gabhale, S. Pandharkar, M. Chaudhari, A. Date, M. Chaudhary, H. Pathan, and S. Jadkar, "Effect of Bath Temperature on Optical and Morphology Properties of CdS Thin Films Grown by Chemical Bath Deposition," Energy Procedia, vol. 110, pp. 202–209, 2017.

[66] H. S. Ahmed, R. Y. Mohammed, and M. H. Khalil, "Effects of Deposition Time And PH on The Characterization of Chemically Synthesized Composite Nano-Wires of Cu2S Thin Films," Sci. J. Univ. Zakho, vol. 9, pp. 184–192, 2021.

[67] C. G. Munce, "Chemical Bath Deposition of Copper Sulfide Thin Films," M.Sc. thesis, Griffith Univ., Queensland, Australia, 2008.

[68] L.-W. Wang, "High Chalcocite Cu2S: A Solid-Liquid Hybrid Phase," Phys. Rev. Lett., vol. 108, art. no. 085703, 2012.

[69] M. Adelifard, H. Eshghi, and M. M. B. Mohagheghi, "Comparative studies of spray pyrolysis deposited copper sulfide nanostructural thin films on glass and FTO coated glass," Bull. Mater. Sci., vol. 35, pp. 739–744, 2012.

[70] A. D. Dhondge, S. R. Gosavi, N. M. Gosavi, C. P. Sawant, A. M. Patil, A. R. Shelke, and N. G. Deshpande, "Influence of Thickness on the Photosensing Properties of Chemically Synthesized Copper Sulfide Thin Films," World J. Condens. Matter Phys., vol. 05, pp. 1–9, 2015.

[71] E. S. Hassan, A. K. Elttayef, S. H. Mostafa, M. H. Salim, and S. S. Chiad, "Silver oxides nanoparticle in gas sensors applications," Journal of Materials Science: Materials in Electronics, vol. 30, no. 17, pp. 15943-15951, 2019.

[72] B. Bharathi, S. Thanikaikarasan, P. Kollu, P. V. Chandrasekar, K. Sankaranarayanan, and S. Shajan, "Effect of substrate on electroplated copper sulphide thin films," J. Mater. Sci. Mater. Electron., vol. 25, pp. 5338–5344, 2014.

[73] Naji and U. Sleman, "Influence of precursor molar ratios on the physical properties of nanocrystalline Cu2−xS thin films prepared by chemical bath deposition method," Chalcogenide Lett., vol. 15, pp. 317–328, 2018.

[74] Y. Guo, Q. Wu, Y. Li, N. Lu, K. Mao, Y. Bai, J. Zhao, J. Wang, and X. C. Zeng, "Copper (i) sulfide: A two-dimensional semiconductor with superior oxidation resistance and high carrier mobility," Nanoscale Horiz., vol. 4, pp. 223–230, 2019.